Photoinduced electron transfer quenching and sugar effects on the electrostatic interaction between an anionic Ru(II) complex and cationic bipyridinium derivatives functionalized w...

ARTICLE *in* INORGANICA CHIMICA ACTA · FEBRUARY 2012

Impact Factor: 2.05 · DOI: 10.1016/j.ica.2011.06.030

3 AUTHORS, INCLUDING:

Joseph R Lakowicz
University of Maryland Medical Center
878 PUBLICATIONS **42,255** CITATIONS

Inorganica Chimica Acta 381 (2012) 104–110

Contents lists available at ScienceDirect

Inorganica Chimica Acta

journal homepage: www.elsevier.com/locate/ica

Photoinduced electron transfer quenching and sugar effects on the electrostatic interaction between an anionic Ru(II) complex and cationic bipyridinium derivatives functionalized with boronic acids

Md. Jamal Uddin [a,*], Nicolas DiCesare [b], Joseph R. Lakowicz [b,*]

[a] Department of Natural Sciences, Coppin State University, 2500 West North Avenue, Baltimore, MD 21216, USA
[b] Center for Fluorescence Spectroscopy, Department of Biochemistry and Molecular Biology, University of Maryland at Baltimore, 725 W. Lombard Street, Baltimore, MD 21201, USA

ARTICLE INFO

Article history:
Available online 24 June 2011

Fluorescence Spectroscopy: from Single Chemosensors to Nanoparticles Science – Special Issue

Keywords:
Electron transfer
Quenching
Sugar
Metal complex
Boronic acid
Spectroscopy

ABSTRACT

The photoinduced electron transfer quenching of an anionic ruthenium(II) metal–ligand-complex $(Ru(dpp(SO_3Na))_2(mcbpy)Cl_2$ by two boronic acid functionalized benzyl viologen (BV^{2+}) derivatives has been investigated as well as their response to sugar. The electrostatic interaction between these two charge species lead to the formation of static quenching which is removed in presence of sugar due to the formation of a neutral zwitterionic quencher. Spectral data, quenching parameters and sugar titration curves are presented and discussed in term of future developments of optical sensors for sugar.

1. Introduction

For a decade, the development of synthetic chemosensors and sensors for the recognition and analysis of sugar has attracted much attention [1–6]. Detection and monitoring of glucose is particularly important for diabetics. The long-term health problems associated with a high blood glucose level show important reduction when diabetics can control and maintain a "normal" blood glucose level. Actual technologies for glucose measurement, mostly based on enzymes and proteins, show important limitations in their uses [7,8]. For example, an implantable sensor for continuous glucose monitoring is expected to find useful applications to help diabetics. To date, none of the actual technologies have been shown to be robust enough for the development of these in-vivo applications. Development of new glucose sensitive materials and new analytical approaches are still needed.

Amount analytical approaches, fluorescence spectroscopy is well known for its promising potential as an analytical tool for in-vivo medical analysis. In addition to its high sensibility and selectivity, fluorescence spectroscopy is a non-invasive method that can be performed in whole blood [9] and through the skin [10]. In addition, actual developments in electronic, in light-emitting devices, and solid-state detectors can lead to simple, low-cost and miniaturized analytical devices that could be used in an automatic and continuously way or used by the patient himself on an hourly schedule.

To date, the most promising chelator group used for the development of synthetics chemosenors for sugar is the boronic acids. Boronic acids form a covalent and reversible interaction with monosaccharides in water. The equilibrium is fast and the affinity and selectivity against different sugars can be enhanced [3,4,11]. Several interesting fluorescence probes functionalized with boronic acids have been developed over the past decade. Mechanisms like photoinduced electron transfer (PET), [11] excited-state charge-transfer [12,13] and molecular rigidification [14], to name a few, have been investigated. While these results are promising, the development of fluorescence probes is a long process, optical responses are hardly predictable and the mechanisms are limited to few fluorophores. In this way, the development of mechanisms that are independent of the nature of the fluorophores are greatly welcome. In this topic, we used change of the boronic acid group, upon binding saccharides, to induce optical changes based on a re-equilibrium of the charged species present [15].

The interaction of the boronic acids with sugar is shortly illustrated in Scheme 1 [16]. Phenyl boronic acids are weak Lewis acids with pK_as ~ 9. The interaction with a diol increases the electrophilicity of the boron group, and typical pK_as ~ 6 are than observed. At

* Corresponding authors. Tel.: +1 410 951 4118; fax: +1 410 951 4110 (Md.J. Uddin), tel.: +1 410 706 8409; fax: +1 410 706 8408 (J.R. Lakowicz).
E-mail addresses: juddin@coppin.edu (Md. Jamal Uddin), lakowicz@umbi.umd.edu (J.R. Lakowicz).

0020-1693/$ - see front matter © 2011 Elsevier B.V. All rights reserved.
doi:10.1016/j.ica.2011.06.030

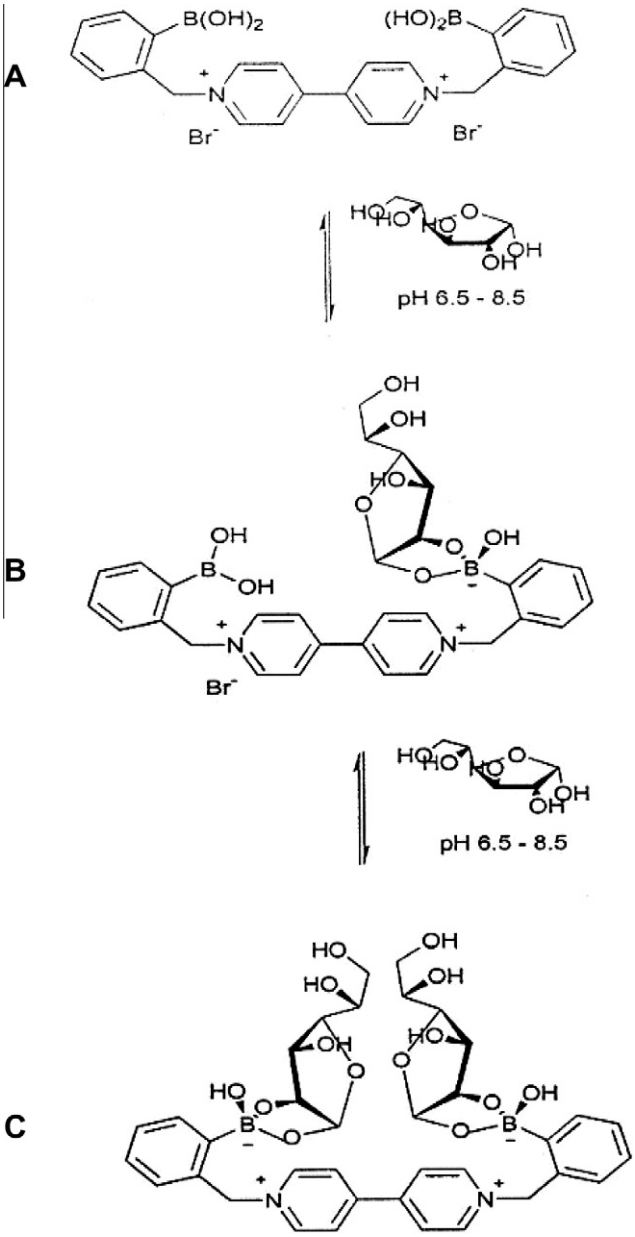

Scheme 1. The interaction of the boronic acids with sugar moiety.

a pH between 6.5 and 8.5, the boronic acid exists under its neutral form (A, Scheme 1) while, in presence of sugars, its exists under its anionic form (B and C, Scheme 1). This change has been first explored by Singaram and collaborators and recently published in a brief communication [15]. In their study, they used a dicationic benzyl viologen quencher functionalized with boroin acids groups (*o*-BV^{2+}, Fig. 1) to quench, by photoinduced electron transfer, the emission of an anionic pyrene derivative following an electrostatic interaction between the two species. In presence of sugar, a neutral zwiterionic quencher is formed (C, Scheme 1), which drawback the formation of complexation between the quencher and the fluorescent probe, and then remove the quenching effect. Using this mechanism, large intensity change can be obtained. Singaram et al. reported intensity increases up to 5-fold using an anionic pyrene derivative, while we reported intensity increases up to 70-fold using an anionic conjugated polymer [17].

In this study, we report the photoinduced electron transfer quenching properties, association constants, and subsequent sugar effect between two benzyl viologen quencher functionalized with

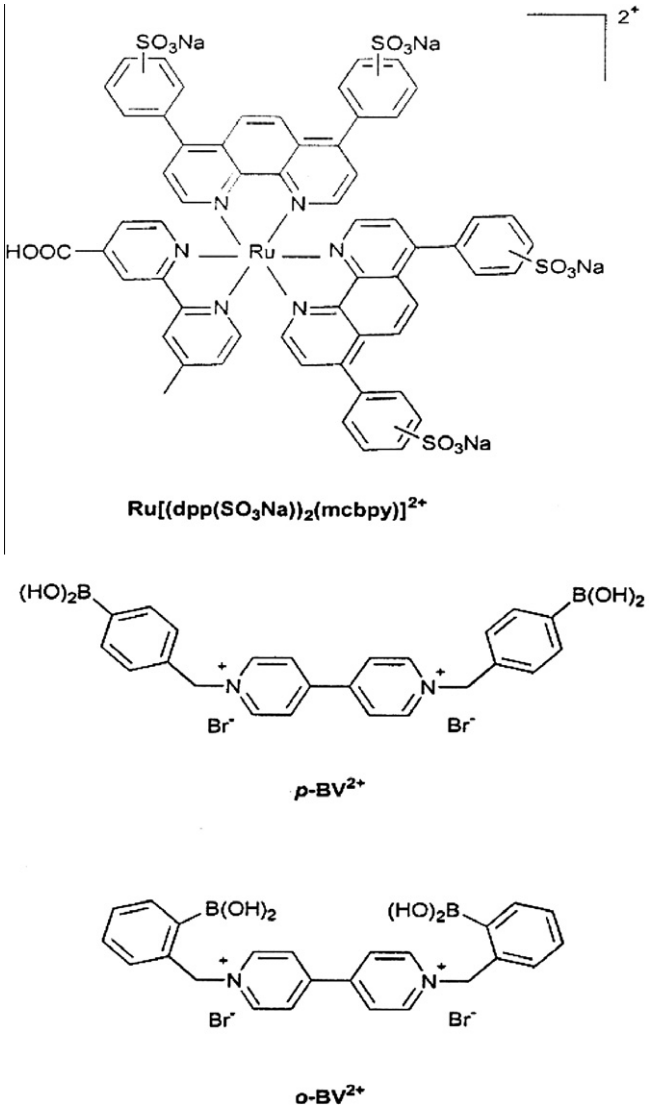

Fig. 1. Molecular structure of the benzyl viologen quenchers with boronic acid groups (*p*-BV^{2+} and *o*-BV^{2+}) and metal–ligand-complex Ru(II)[(dpp$(SO_3Na)_2)_2$-(mcbpy)]Cl_2.

boronic acid groups (*p*-BV^{2+} and *o*-BV^{2+}, Fig. 1) and an anionic ruthenium(II) metal-ligand-complex (MLC) (Fig. 1). Ru MLC are today known for their good spectrum characteristics (photo-stability, large Stokes' shift, long-wavelength emission, long-lifetime, etc.) and are very promising as active material for the elaboration of optical sensors [18].

In addition, Ru^{II}–polypyridyl complexes show sensitivity to the presence of bipyridinium derivative through an oxidative electron-transfer acceptor dipyridium [19–21].

The Stern–Volmer constants (K_{SV}) obtained from steady-state and time-dependent measurements and super linear quenching is discussed in terms of static quenching and sphere of action model. Consequence of the presence of sugar on the K_{SV} and static quenching is also presented and discussed as well as the effect of the ionic strength of the solution on these parameters. Sugar titration curves are presented and discussed in terms of future development of optical sensors based on this mechanism.

2. Experimental materials

All solvents (HPLC grade), methyl viologen (MV^{2+}) and starting chemicals for the synthesis were from Aldrich and used as re-

ceived. D-fructose, D-galactose and D-glucose were purchased from Sigma. Ru(dpp(SO_3Na)$_2$)$_2$(mcbpy)Cl_2 [22], 2-(4-bromomethyl-phenyl)-5,5-dimethyl-(1,3,2)dioxaborinane [23] and 2-(2-bromomethyl-phenyl)-5,5-dimethyl-(1,3,2)dioxaborinane [11] were obtained as described in the literature. The ortho derivative, *o*-BV^{2+}, was synthesized according to a slightly different procedure than reported in the literature [15].

2.1. 4,4′-N,N′-Bis(benzyl-2-boronic acid-bipyridinium dibromide (*o*-BV^{2+})

4,4-Dipyridyl (375 mg, 2.4 mmol) and 2-(2-bromomethyl-phenyl)-5,5-dimethyl-(1,3,2)dioxaborinane (1.5 g, 5.3 mmol) were heated to reflux in CH_3CN (25 ml) for 4 h. After cooling to room temperature, the resulting yellow precipitate was recovered by filtration and washed with acetone. Without further purification, the solid was dissolved in an H_2O/MeOH solution and extracted for two days with ethyl acetate. After separation, the aqueous solution was concentrated and the product was precipitated by the addition of acetone, giving 871 mg (62%) of a pale yellow solid. Analytical and spectroscopic measurements are in accordance with those published [15].

2.2. 4,4′-N,N′-Bis(benzyl-4-boronic acid)-bipyridinium dibromide (*p*-BV^{2+})

The *para* derivative, *p*-BV^{2+}, was synthesized according to the procedure described above, starting with 2-(4-bromotheyl-phenyl)-5,5-dimethyl-(1,3,2)dioxaborinane, giving a yellow solid (74%), mp 236–237 °C (decomp.). (300 MHz; CD_3OD) 6.00 (4H, s, CH2), 7.59 (2H, d, J = 7 Hz, PhH), 7.76 (2H,d, J = 7 Hz, PhH), 8.70 (2H, d, J = 6hz, ArH), 9.38 (2H, d, J = 6 Hz, ArH). *m/z* (EI) 485 (M^+, 100%). *Anal.* Calc. for $C_{24}H_{24}B_2Br_2N_2O_4$ (585.9): C, 49.20; H, 4.13; N 4.78. Found: C, 48.76; H, 4.5; N, 4.67%.

3. Method and instrumentation

Absorption and emission spectra were recorded with a Cary 50 UV–Vis spectrophotometer (Varian Inc.) and a Eclipse Spectrofluorometer (Varian Inc.), respectively. In all cases, the measurements were taken at room temperature in a 1-cm quartz cuvette under an air atmosphere. For all measurements, the absorbance of the solutions were around 0.1 at the excitation wavelength.

The quenching studies were done by taking the emission spectrum of the solution at a series of quencher concentration and comparing the photoluminescence intensities (I). Stern–Volmer constants (K_{SV}) were obtained by linear fitting the experimental data according to the relation:

$$\frac{I_0}{I} = 1 + K_{SV}[C] \tag{1}$$

where I_0 is the photoluminescence in absence of quencher and (C) the concentration of quencher. Titration curves against sugar were fitted and dissociation constant (K_D) values were obtained using the relation:

$$I = \frac{I_0 + I_f K_D^{-1}[C]^n}{1 + K_D^{-1}[C]^n} \tag{2}$$

where I_0 and I_f are the initial (no sugar) and final (plateau) intensities of the titrations curves. In case of an apparent 1:1 complexation model, n = 1, and in the case of an apparent 1:2 complexation model, n = 2.

Frequency domain (FD) measurements were performed using the instrumentation described previously [24–26]. Excitation was provided by a blue LED (450 nm, Nishia Co.) through a blue filter (Corning 4303) to remove the long-wavelength emission component from the LED. Emission was observed through a combination of a cut-off (550 nm) and an interference filter (615 nm + 25 nm) to remove scattered and Raman scattered light. The measurements were taken in a 1-cm cuvette under an air atmosphere. The frequency intensity profiles were analyzed by nonlinear least squares in terms of the multi-exponential model:

$$I(t) = \sum_i \alpha_i \exp(-t/\tau_i) \tag{3}$$

where α_i is the pre-exponential factor associated with the decay time τ_i, with $\sum_i \alpha_i$ = 1.0. The mean lifetime is given by:

$$\overline{\tau} = \frac{\sum \alpha_i \tau_i^2}{\sum \alpha_i \tau_i} = \sum f_i \tau_i \tag{4}$$

where f_i is the fractional steady-state intensities of each lifetime component.

$$f_i = \frac{\alpha_i \tau_i}{\sum_j \alpha_j \tau_j} \tag{5}$$

Errors of 0.5 and 0.01 on the phase angle and modulation have been used, respectively.

4. Results and discussion

Fig. 2 displays the absorption and emission spectra of the Ru-MLC investigated as well as the absorption spectrum of *p*-BV^{2+}. Both quenchers, *p*-BV^{2+} and *o*-BV^{2+}, show identical absorption profiles. The MLC was excited through its metal-ligand-charge-transfer (MLCT) transition at 460 nm. At this wavelength, both benzyl viologen derivatives do not show any significant absorbance.

For all measurements, the absorption spectrum was recorded after the complete addition of the quencher, and in all cases, no change in the spectrum was observed (Fig. 3), except at shorter wavelengths than 375 nm where the quenchers show absorption.

This result is in contrast with the results reported by Singaram et al. where they observed changes in the absorption spectrum of an anionic pyrene derivative upon complexation with *o*-BV^{2+}. Obviously, the nature of the MLCT transition is not perturbed upon complexation with the quenchers.

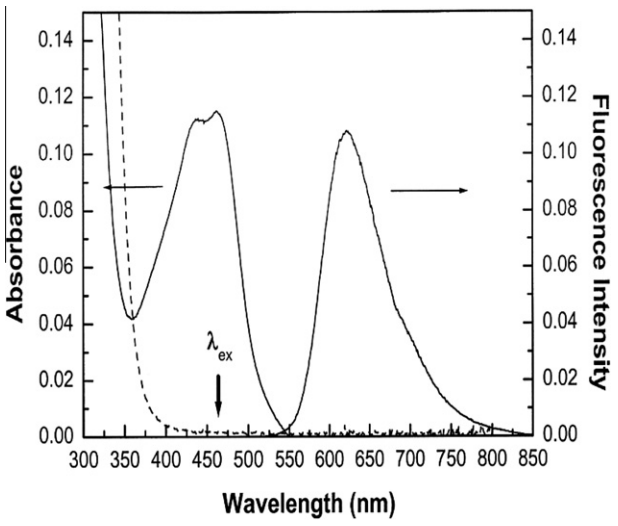

Fig. 2. Absorption and emission spectra of the Ru(II) metal–ligand-complex along with the absorption spectrum of *p*-BV^{2+}.

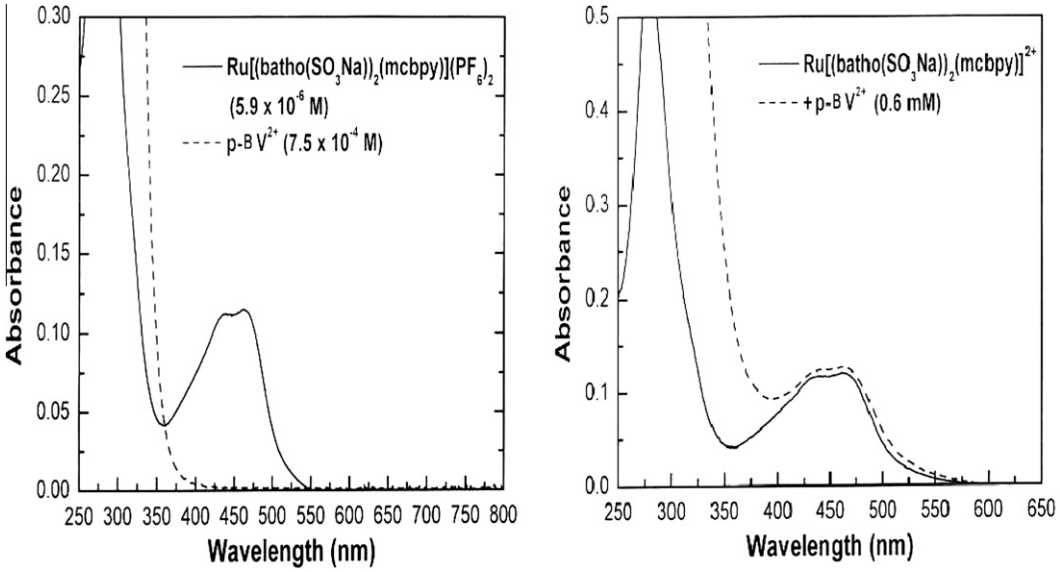

Fig. 3. Absorption spectra of Ru-MLC, the *p*-BV^{2+} quencher (left) and the addition of the Ru-complex + *p*-BV^{2+} quencher (right).

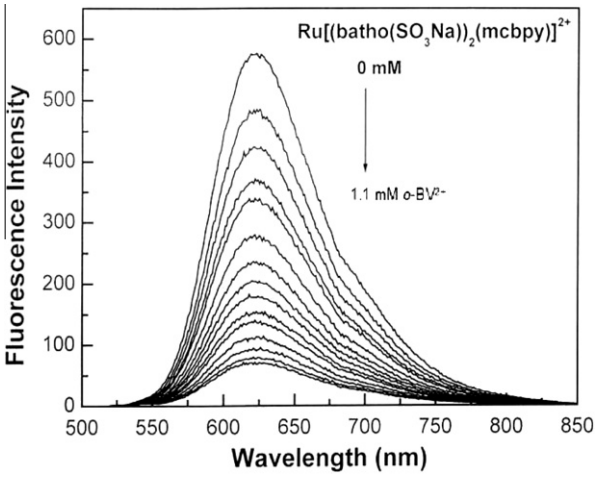

Fig. 4. The spectral response of the Ru-MLC as the concentration of *o*-BV^{2+} increase.

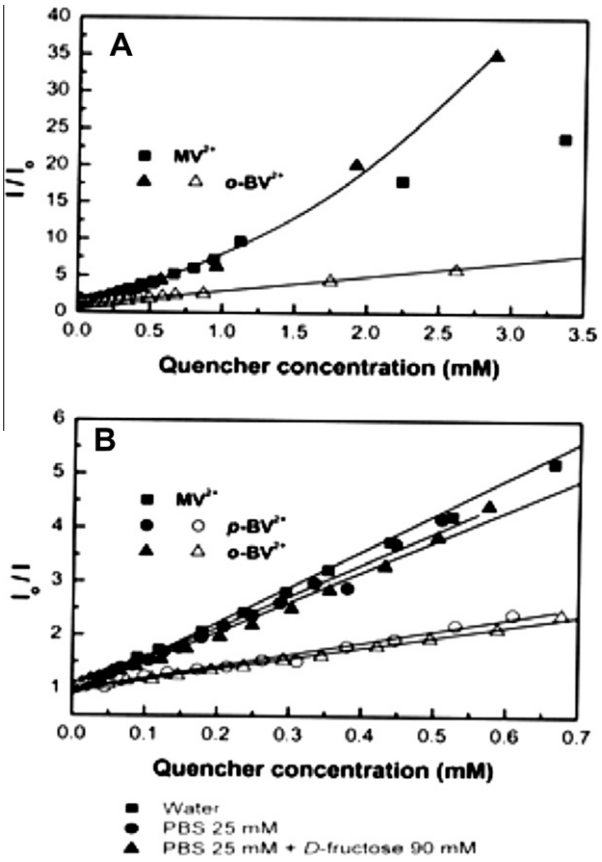

Fig. 5. Stern–volmer plots for Ru-MLC and *o*-BV^{2+} quencher in water and PBS at RT (absence and presence of sugar).

Fig. 4 shows the spectrum response of the Ru-MLC as the concentration of *o*-BV^{2+} increase. Corresponding Stern–Volmer plots are displayed in Fig. 5A. As the concentration of quencher increase, we observe a large decrease of the luminescence of the Ru-MLC with no apparent shift. At low concentration of quencher, the Stern–Volmer plots show linear relation with the concentration (Fig. 5B). Both benzyl viologen derivative functionalized with the boronic acid group show similar Stern–Volmer constant as methyl viologen (MV^{2+}), showing that the presence of the benzyl and the boronic acid groups does not alter the quenching property of the viologen moiety. Quenching rate constants (k_q) calculated are one order higher than the quenching rate constant reported for the system $Ru(bpy)_3^{2+}/MV^{2+}$ ($k_q = 0.74 \times 10^{-9}\ m^{-1}\ s^{-1}$) [22]. Since diffusion coefficient is expected to be similar in both systems, the higher quenching rate constant are expected due to the specific interaction between the anionic Ru-MLC and the cationic quencher. This quenching rate constant can be enhanced by increasing the number of negative charge on the MLC. For example, a Ru-MLC bearing four negative charges shows a quenching rate constant of $10.1 \times 10^{-9}\ M^{-1}\ S^{-1}$. The MLC reported in this work (Fig. 1) posses two negative charges, if the carboxylic acid group is considered non-ionized.

At a higher concentration of quencher, an upward curvature of the Stern–Volmer plot is observed showing the presence of static

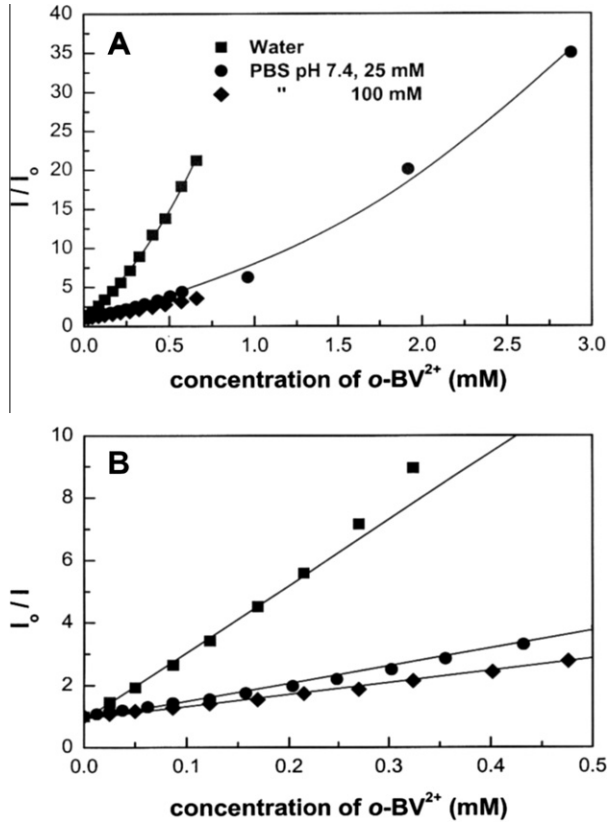

Fig. 6. Stern–volmer plots for Ru-MLC and *o*-BV^{2+} quencher in water and PBS at RT. (Note the linear pattern for low concentrations.)

quenching. The Stern–Volmer profile at a high concentration of *p*-BV^{2+} is not shown due to the low solubility of *p*-BV^{2+} in phosphate buffer solution.

Since the amplified quenching comes from an electrostatic interaction between the luminophore and the quencher, it strongly depends on the ionic strength of the media.

Fig. 6 shows the effect of the concentration of the phosphate buffer solution (PBS) on the Stern–Volmer profiles. In water, a large Stern–Volmer constant was obtained, while in presence of PBS, 25 mM, the quenching constant shows a decrease of about 4-fold. This decrease continues as the concentration of PBS increases as shown in Fig. 7.

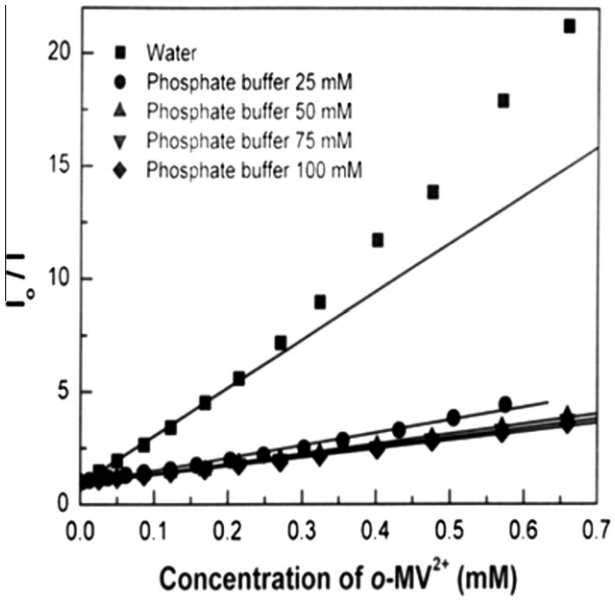

Fig. 7. Stern–volmer plots for the effect of concentration of PBS at RT.

Due to the limited solubility of the quencher at a high concentration of PBS, we were not able to observe whether the upward curvature at a high concentration is maintained or not.

Dynamic (K_D) and static (K_S) quenching constants were evaluated using the theory of static quenching, both constants were obtained from the slope and intercept of a plot of $((I_0/I) - 1)/(Q)$ vs (Q) [23]. In water, a dynamic quenching constant of 16200 M^{-1} was obtained with a static quenching constant of 1280 M^{-1}. Both dynamic and static quenching constants were reduced in the presence of PBS 25 mM, $K_D = 3400\ M^{-1}$ and $K_S = 800\ M^{-1}$. Since the static constant represents the stability constant of the complex luminophore/quencher, the results show that in the PBS solution the formation of complexes is greatly reduced.

Fig. 8 shows the frequency domain intensity decays of Ru-MLC is decreased from 740 ns to 135 ns in H_2O by adding 0.43 mM *p*-BV^{2+} quencher. We also investigated the effect of adding D-fructose on the FD intensity decays of Ru-MLC and the quenchers in PBS at RT. The lifetime of Ru-MLC has decreased to 282 ns in the presence of 40 mM D-fructose. The change of the life time is relatively small, more studies are on the way to link this decrease of lifetime with electronic properties involved in the molecule following the binding with sugars and the formation of the anionic form. Fig. 9 shows the Stern–Volmer plots of F–D intensity decays for Ru-MLC and *p*-BV^{2+} quencher in H_2O and PBS. The plots are shown the linearity at lower concentration. The Dynamic quenching constants obtained using this model and the steady-state intensity are in agreement with those obtained with the time-decay measurements, Figs. 8 and 9.

5. Are the dynamic quenching constants supposed to be the same in water and in PBS 25 mM?

In the presence of D-fructose, D-fructose was chosen due to its higher affinity to monoboronic acid derivative [11], the quenching properties of the boronic acid functionalized benzyl viologen derivatives are reduced (Fig. 5). Stern–Volmer constants are reduced to ~2.8-fold and super linear quenching are suppressed at a higher concentration of quencher. This reduction of the quenching is due to the formation of a neutral zwiterionic viologen derivative, C Scheme 1. The ionic complexation between the anionic Ru-MLC and the neutral quencher are expected to be removed, resulting only in quenching from diffusion.

This difference in the quenching property of the boronic acid functionalized benzyl viologen derivatives in the presence of sugar can be used to monitor the sugar concentration in the solution. In this case, at a selected and fixed quencher concentration, amplified quenching can be observed in the absence of sugar, while in the presence of sugar, this quenching is removed and the intensity increases are observed. To study the sugar profile response of both benzyl viologen derivatives, we used a quencher concentration of 0.5 mM in a PBS pH 7.4 at concentration 25 mM. While these conditions are far to be optimized to show the highest sugar response, we chose these conditions, first because of the relatively low solubility of the quenchers and also to have a non-zero ionic strength solution since potential applications will virtually be useful in biological media. Both the quencher concentration and ionic strength of the solution greatly affect the optical response of the system. As shown on Fig. 5A, very large intensity changes, between the absence and the presence of sugar can be obtained at a higher concentration of quencher in the upward curvature of the Stern-Volmer plot. Also as seen in Fig. 6A, this upward curvature increase as the ionic

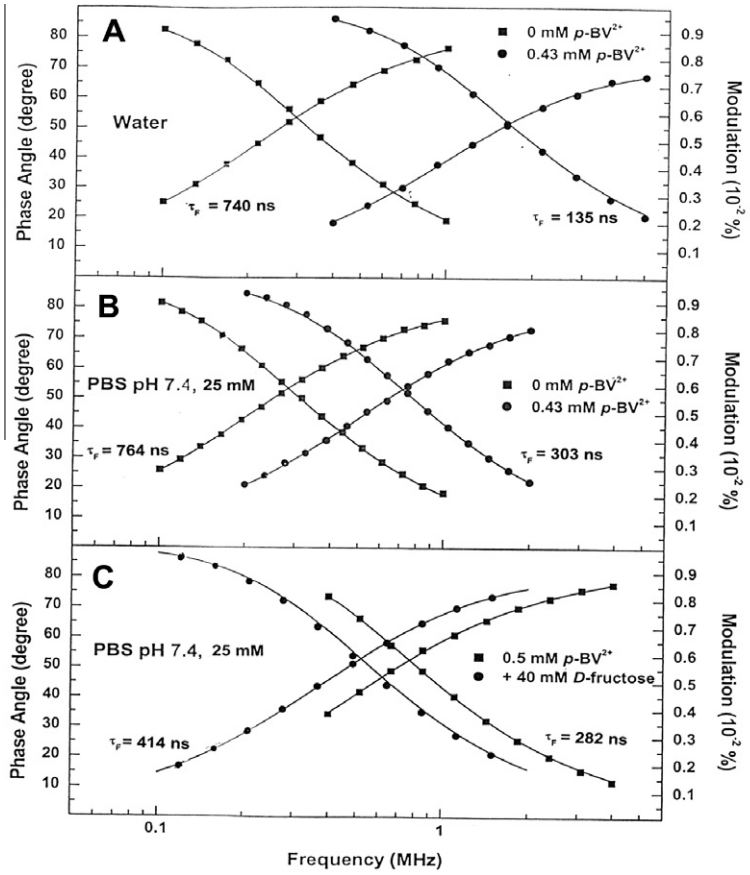

Fig. 8. Frequency domain intensity decays of Ru-MLC and p-BV^{2+} quencher in water and PBS at RT (absence and presence of sugar).

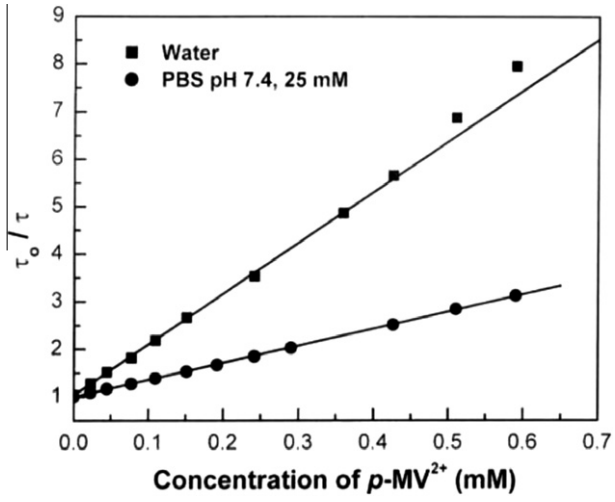

Fig. 9. Stern–volmer plots of FD intensity decays for Ru-MLC and p-BV^{2+} quencher in water and PBS at RT.

strength of the media decreases. By carefully tuning these parameters, it would be possible to optimize the spectral response of the system.

6. Conclusion

The photoinduced electron transfer (PET) quenching reaction of metal–ligand-complex Ru(II)[(dpp$(SO_3Na)_2)_2$(mcbpy)]Cl_2 in aqueous solution have been studied by using two boronic acid functionalized benzyl viologen (BV^{2+}) derivatives as quenchers. The subsequent sugar effect is reported between this two quenchers and ruthenium(II) metal–ligand-complex. The combination of electron withdrawing and/or donating group and boronic acid group both directly linked to Ru MLC could lead to the formation of an excited ^{3}MLCT state. After complexation with a sugar molecule boronic acid changes from the neutral form to the anionic one and a change in the MLCT properties of the Ru MLC occurs. A drastic change in the fluorescence intensity has been observed as the concentration of quenchers increased. This leads to a new optical and ratio metric approach for the analysis of sugar molecule using MLC probes having the boronic acid group.

Acknowledgements

This work has been supported by the Juvenile Diabetes Foundation International, 1-2000-546, and by the NIH National Center for research Resources, RR-08119.

References

[1] T.D. James, S. Shinkai, Host–Guest Chemistry, in: Topics in Current Chemistry, vol. 218, Springer-Verlag, Berlin, 2002, p. 159.
[2] J.H. Hartley, T.D. James, C.J. Ward, J. Chem. Soc., Perkin Trans 1 19 (2001) 3155.
[3] H. Eggert, J. Fredericksen, C. Morin, J.C. Norrid, J. Org. Chem. 64 (1999) 3846.
[4] W. Yang, H. He, D.G. Drueckhammer, Angew. Chem., Int. Ed. 40 (2001) 1714.
[5] S. Gao, W. Wang, B. Wang, Bioorg. Chem. 29 (2001) 308.
[6] N. Dicesare, J.R. Lakowsicz, J. Chem. Soc., Chem. Commun. 19 (2001) 2022.
[7] A. Heller, Annu. Rev. Biomed. Eng. 1 (1999) 153.
[8] D.A. Gough, J.C. Armour, Diabetes 44 (1995) 1005.
[9] O. Abugo, P. Hermann, J.R. Lakowicz, SPIE Proc. 3913 (2000) 145.
[10] S.B. Bambot, G. Rao, M. Romauld, G.M. Carter, J. Sipior, E. Terpetching, J.R. Lakowicz, Biosens. Bioelectron. 10 (1995) 643.

[11] T.D. James, K.R.A.S. Sandanayake, R. Iguchi, S. Shinkai, J. Am. Chem. Soc. 117 (1995) 8982.
[12] H. Shinmori, Tetrahedron 51 (1995) (1893).
[13] N. DiCesare, J.R. Lakowicz, J. Phys. Chem. A 105 (2002) 6834.
[14] M. Takeuchi, T. Mizuno, H. Shinmore, M. Nakashima, S. Shinkai, Tetrahedron 52 (1996) 1195.
[15] J.N. Camara, J.T. Suri, F.E. Cappuccio, R.A. Wesling, B. Singaram, Tetrahedron Lett. 43 (2002) 1139.
[16] J.P. Lorand, J.O. Edwards, J. Org. Chem. 24 (1959) 769.
[17] N. DiCesare, J.R. Lakowicz, in preparation.
[18] J.R. Lakowicz, Principles of Fluorescence Spectroscopy, Kluwer Academic/Plenum Press, second ed., New York, 1999, p. 573.
[19] C.R. Bock, T.J. Meyer, D.G. Whitten, J. Am. Chem. Soc. 96 (1974) 7410.
[20] K. Kalyanasundarum, Coord. Chem. Rev. 42 (1982) 159.
[21] R. Lomoth, T. Haupl, O. Johanson, L. Hammerstrom, Chem. Eur. J. 8 (2002) 102.
[22] A. Yoshimura, M.J. Uddin, N. Amasaki, T. Ohno, J. Phys. Chem. A 105 (2001) 10846.
[23] J.R. Lakowicz, Principles of Fluorescence Spectroscopy, Kluwer Academic/Plenum Press, second ed., New York, 1999, p. 242.
[24] H. Szmacinski, F.N. Castellano, E. Terpetsching, J.D. Dattelbaum, J.R. Lakowicz, G.J. Meyer, Biochim. Biophys. Acta, Protein Struct. 1383 (1998) 151.
[25] N. DiCesare, J.R. Lakowicz, J. Photochem. Photobiol. A 143 (2001) 39.
[26] J.R. Lakowicz, I. Gryczynski, Topics in Fluorescence Spectroscopy, vol. 1, Plenum Press, New York, 1991, p. 293.